Nanoscale

Accepted Manuscript

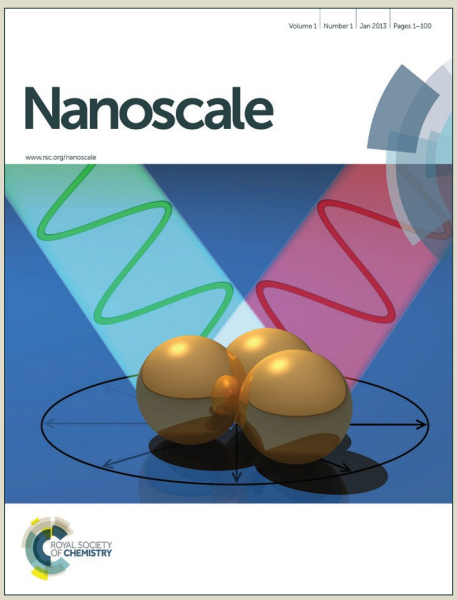

ROYAL SOCIETY OF CHEMISTRY

www.rsc.org/nanoscale

Journal Name

RSCPublishing

COMMUNICATION

Investigation of Cyano-Bridged Coordination Nanoparticles $Gd^{3+}/[Fe(CN)_6]^{3-}$/D-mannitol as a T_1-weighted MRI Contrast Agent.

Cite this: DOI: 10.1039/x0xx00000x

Received 00th January 2012,
Accepted 00th January 2012

DOI: 10.1039/x0xx00000x

www.rsc.org/

M. Perrier,[a†] A. Gallud,[b†] A. Ayadi,[c] S. Kenouche,[c] C. Porredon,[d] M. Gary-Bobo,[b*] J. Larionova,[a*] Ch. Goze-Bac,[c] M. Zanca,[c,e] M. Garcia,[b] I. Basile,[f] J. Long,[a] J. de Lapuente,[d] M. Borras,[d] and Y. Guari[a]

Cyano-bridged $Gd^{3+}/[Fe(CN)_6]^{3-}$ coordination polymer nanoparticles of 3-4 nm stabilized by D-mannitol presenting high r_1 relaxivity value of 11.4 $mM^{-1}s^{-1}$ were investigated *in vivo* as contrast agents (CA) for Magnetic Resonance Imaging (MRI). They permit an increase of the MR image contrast and can act as an efficient intravascular T_1 CA with a relatively long blood-circulation lifetime (60 min) without specific toxicity.

Coordination polymers at the nanoscale is an exciting new class of nanomaterials whose origin is the infinite bulk molecule-based networks and that present tuneable size- and shape- dependent properties, a high surface area to volume ratio and tailored functionalized surfaces.[1] Therefore, they exhibit unique physical and chemical properties which are interesting not only for the fundamental aspect, but also because of their intended use in various technological applications with a great potential in biology and medicine.[2] Several examples of nano-sized Metal-Organic Frameworks (MOFs) or cyano-bridged coordination polymers were found promising as drug delivery nano-carriers,[3] as therapeutic agents[4] or as CAs for various type of imagery.[5] Among those, a particular development of coordination network nanoparticles was devoted to design new CAs for Magnetic Resonance Imaging (MRI) because they not only can compete with commercial contrast agents (CAs) in terms of MRI efficiency but also because they can exhibit a different behaviour particularly in terms of circulation time and biodistribution.[6]

MRI is a powerful non-invasive technique widely used in clinical practices based on the mechanism of Nuclear Magnetic Resonance (NMR) and the relaxation of hydrogen proton spins in an applied magnetic field. Various positive (T_1-weighted) CAs, mainly based on paramagnetic Gd^{3+} chelates, or negative (T_2-weighted) superparamagnetic iron oxides nanoparticles are used to improve the image contrast between healthy and pathological tissues of the human body. An increased relaxivity allows the CAs to be administered at a lower dose or permits imaging low-concentration targets which remains a major challenge of modern medical research. A promising strategy to achieve an efficient MRI positive CA is to design a relatively small (< 5.5 nm) Gd^{3+}-containing nano-object that increase the local Gd^{3+} concentration in the region of interest and decrease the tumbling time due to the high molecular weight and rigidity thus leading to an increased relaxivity. In this line of thought, GdF_3,[7] gadolinium oxides,[8] gadolinium phosphates[9] or $Gd(IO_3)_3$ nanoparticles,[10] Gd^{3+}-based MOF's nanorods,[6a-c] citrate coated Gd^{3+}-doped Prussian blue nanoparticles[11] or $KGd(H_2O)[Fe(CN)_6]$ nanoparticles[12] presenting higher r_1 relaxivity in comparison with commercial (for instance ProHance@ or Magnevist@) CAs were reported. We recently investigated Gd^{3+}-based cyano-bridged coordination polymer nanoparticles coated with a biopolymer chitosan and having a longitudinal relaxivity at least six times higher than that of T_1-relaxing commercial CAs but with a stability limitation at physiological pH due to chitosan itself.[13], [14] Most recently, we completed this family of nanoparticles by developing nano-sized cyano-bridged coordination polymers nanoparticles coated with water soluble at physiological pH PEG or sugar derivatives, which revealed also interesting as positive CA regarding their high r_1 values. This study was devoted to the synthesis of the nanoobjects and investigation their NMR relaxivity properties, which depend on the spin value of the lanthanide ion, the presence of the second transition ion in the nanoparticles network or the optimal size of the nanoparticles.[15] In this communication, we report on $Gd^{3+}/[Fe(CN)_6]^{3-}$ nanoparticles stabilized by biocompatible and water soluble stabilising agent D-mannitol, that exhibit r_1 relaxivity four times higher than commercial CAs and demonstrate for the first time that they can act *in vivo* as an efficient intravascular T_1 MRI CA without presenting specific toxicity.

The $Gd^{3+}/[Fe(CN)_6]^{3-}$@D-mannitol nanoparticles were obtained by the stoichiometric reaction between $Gd(NO_3)_3.6H_2O$ and $Na_3[Fe(CN)_6]$ in water in the presence of D-mannitol as a stabilizing agent (SI for Experimental, Scheme S1). The nanoparticles were then centrifuged to remove any precipitate that may form and the supernatant was filtered on a 0.45 μm filter. The resulting nanoparticles' solution was purified from the excess stabilizing agent, the $NaNO_3$ salt formed during the reaction and possible unreacted molecular precursors by precipitation with acetone, centrifugation and several washing with

ethanol. The elemental analysis permits to determine that the Gd^{3+}/Fe^{3+} ratio is 1, the expected value for the bulk compound of formula $Gd(H_2O)_4[Fe(CN)_6]$[16] and that there is no trace of Na^+ which excludes the presence of this monocation inserted into the structure or traces of $NaNO_3$ salt as an impurity. InfraRed spectroscopy confirmed the formation of the cyano-bridged network as demonstrated by the higher wavenumber values in the cyanide stretching region (2150, 2139, 2108, 2065 cm^{-1}) in comparison with the ferricyanide precursor used. The X-Ray diffraction pattern (Fig. S1, SI) is comparable to the one of the bulk $Gd(H_2O)_4[Fe(CN)_6]$ which crystallizes in an orthorhombic system with a *Cmcm* space group.[16] Note that in such a structure, the Gd^{3+} site is octacoordinated and surrounded by six cyano-bridging groups and two coordinated water molecules capable of exchange with bulk water (Fig. 1). Transmission Electronic Microscopy (TEM) measurements performed from aqueous solutions of these nanoparticles show the presence of non-aggregated spherical nanoparticles with a mean size distribution of 3.41 ± 0.45 nm (Fig. 1) which, taking into account the cell parameters allows to estimate the number of Gd^{3+} and Fe^{3+} paramagnetic ions and leads to a chemical composition $\{Gd(H_2O)_4[Fe(CN)_6]\}_{66\pm9}$.

The room temperature proton T_1 and T_2 relaxation time measurements were performed for aqueous solutions of nanoparticles with different concentrations at an applied magnetic field of 4.7 T by using a spectrometer Tecmag Apollo operating at 200 *MHz*. The longitudinal, r_1, and transverse, r_2, relaxivities were determined from the slopes of the plot of $1/T_1$ and $1/T_2$ *vs* nanoparticles' concentration and are equal to 11.4 ± 0.1 and 12.6 ± 0.1 $mM^{-1}s^{-1}$ (Fig. S2, SI) with a r_2/r_1 ratio equal to 1.01. These values are four times larger than the ones obtained for the commercial CA Gadoteridol known as the trademark Prohance@ (3.00 ± 0.01 and 3.41 ± 0.01 $mM^{-1}s^{-1}$ for r_1 and r_2, respectively (Fig. S3, SI)). Furthermore, the r_2/r_1 ratio is close to 1, as required for efficient *T1* CA. The relatively high r_1 value may be rationalized in light of the structural aspects of $Gd(H_2O)_4[Fe(CN)_6]$ coordination network as well as of the nanoparticules' size: (*i*) the cyano-bridged network containing two water molecules coordinated to Gd^{3+} sites that can be exchanged with the bulk water solvent (Fig. 1); (*ii*) the small size of nanoparticles of 3.41 nm, which implies that around 35 % of ions are located at the surface making these Gd^{3+} site particularly accessible to water; (*iii*) the tumbling time for the nanoparticles which should increase to about the nanosecond in comparison with the Gd^{3+} chelates (in the picosecond range); (*iv*) the presence of magnetic interactions between Gd^{3+} and Fe^{3+} ions through the cyanide bridge visibly still operating at room temperature that also helps to increase the relaxivity.[15]

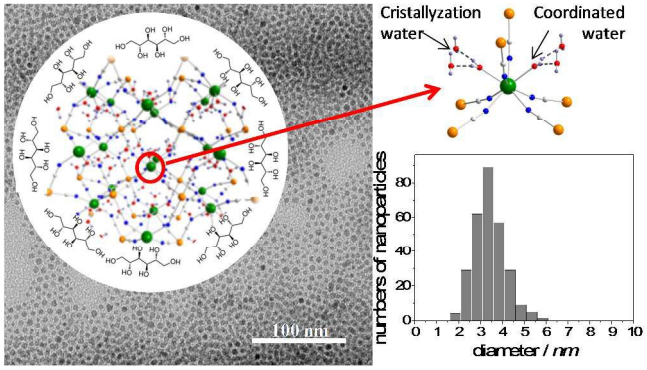

Figure 1. left) Transmission Electronic Microscopy (TEM) image of $Gd^{3+}/[Fe(CN)_6]^{3-}$@D-mannitol and (inset) their schematic representation; right up) Gd^{3+} site with coordinated and crystallized water molecules which can be exchanged with solvent water ; right down) nanoparticles' size distribution histogram.

Before use for *in vivo* imaging, the stability and cytotoxicity of the $Gd^{3+}/[Fe(CN)_6]^{3-}$@D-mannitol nanoparticles as well as the viability of mice after nanoparticles' injection were tested. The nanoparticles stability in time was evaluated in 40 % fetal bovine serum (FBS) by TEM and by monitoring the relaxivities. The shape of the nanoparticles as well as the size does not show any sign of evolution after 1 month (Fig. S4, SI). The r_1 and r_2 values remain stable over the period of one week, indicating that no nanoparticles decomposition or aggregation occurs. Cytotoxicity was first evaluated on human colorectal carcinoma cell line HCT-116 and normal human fibroblasts by exposing these for 3 days to a concentration range of nanoparticles from 0.1 to 50 $\mu g.mL^{-1}$. A low cytotoxicity appears for fibroblasts incubated cells from a nanoparticles' concentration of 20 $\mu g.mL^{-1}$ ($5.0 \cdot 10^{-5}$ $mol.L^{-1}$), while no obvious decrease of cell viability is observed for HCT-116 cells (Fig. S5, SI). Safety evaluation were performed and demonstrated that nanoparticles did not present carcinogenic effect in the studied conditions (Fig. S6, SI). Moreover, the *in vivo* toxicity performed over 16 days by intravenous injection with a dose of 0.012 mmol of nanoparticles per kg indicates good viability of the mice (100 %) for all groups reflecting the low toxicity of the nanoparticles (Fig. S7).

130 µL of a NaCl solution containing $Gd^{3+}/[Fe(CN)_6]^{3-}$@D-mannitol nanoparticles at a concentration of $2.4 \cdot 10^{-2}$ $mol.L^{-1}$ were injected intravenously as a bolus in the tail vein of anesthetised healthy mice (6 months, male), which corresponds to 0.003 mmoles of Gd^{3+} per kg to obtain *in vivo* MRI images. T_1-weighted MR images were acquired before and after injection at different times. Two sets of images (top and bottom) corresponding to two different coronal slices of mice before injection (a), 20 min after injection (b) and the summated images after one hour for the organs of interest (c) are shown in Fig. 2. A significant T_1-weighted signal enhancement was clearly observed after 20 min in the heart, the aorta, the liver, the vessels, the veins leading to the bladder (Fig. 2, top), the vena cava and the kidneys (Fig. 2, bottom) owing to the high r_1 relaxivity of the nanoparticles. After 60 min, the signal intensity starts to decrease especially in the bladder and the liver veins and the vena cava (Fig. S8 and S9, SI). The bright signal of the blood pool indicates that these nanoparticles can flow in the vessels without an obvious uptake by the

reticuloendothelial system (*i.e.* liver and spleen) for a relatively long period of time (60 min.) and can therefore be used as intravascular MR contrast agent. In comparison, the injection of the Gd-DTPA even at much higher dose of 0.02 mmoles Gd^{3+} per kg induced only a discrete signal enhancement due to its lesser effect on the proton relaxivity of water compared to the nanoparticles, but also its fast excretion from the body through glomerular filtration clearance (around 20 min.).[17] The MRI dynamic quantification is shown in Fig. 3 as a variation of the mean nanoparticles concentration per voxel as a function of time per organ of interest (heart, bladder, kidney, vena cava). For all organs except bladder, the nanoparticles' concentration presents an exponential decay with a maximum at 20 minutes. The maximal concentration of the CA is found in the vena cava indicating its particular affinity with the liver, which may be explained by the presence of D-mannitol at the nanoparticles surface. For the bladder, the concentration increases very slowly to reach a maximum after 60 minutes and then begins to decrease. These facts suggest that both, the faeces and the glomerular clearing may be involved in the nanoparticles elimination. Time-dependent evolution of Gd^{3+} concentration in blood, extracted from dynamic acquisitions in a region of interest (ROI) placed upon the vena cava, was fitted with a bi-compartmental model (Fig. S10, SI). Then the "effective injected dose" of contrast medium of about 0.06 μmol ($6•10^{-7}$ mol) was determined from the vena cava ROI presenting a volume of about 320 voxels (about $9.16•10^{-6}$ ml).

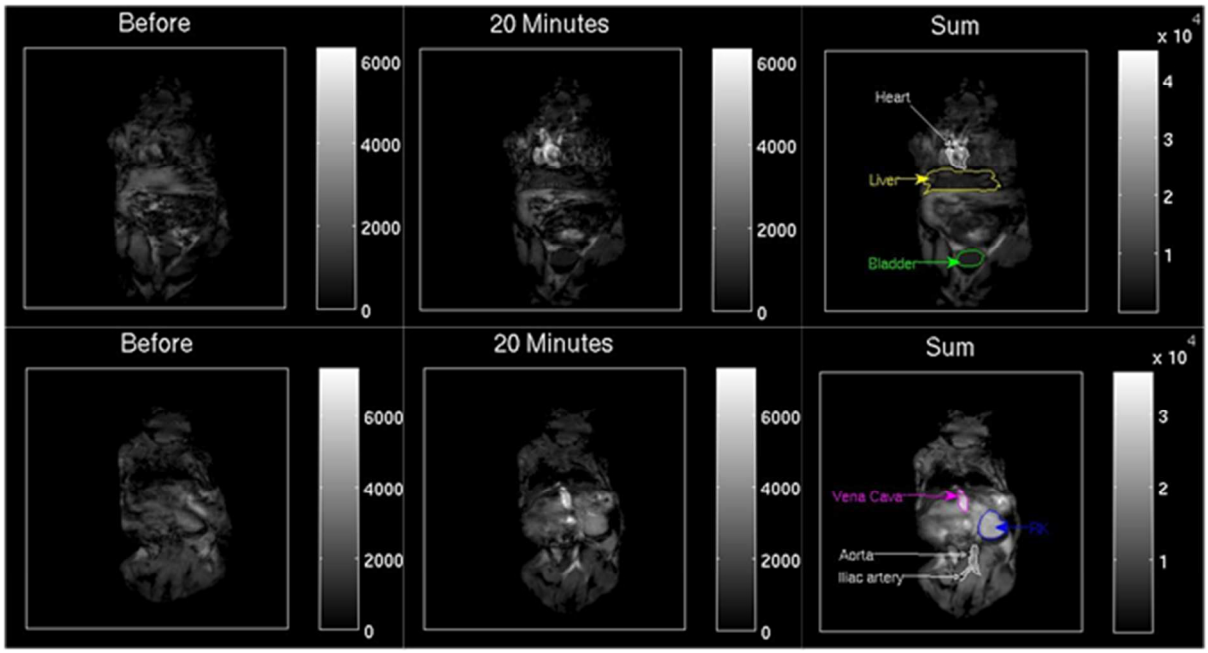

Figure 2. T_1-weighted images of coronal slices of mice acquired before nanoparticles intravenous $Gd^{3+}/[Fe(CN)_6]^{3-}$/D-mannitol injection (a), 20 min after injection (b), and the summated images of the organs of interest (c). Top: coronal slices showing heart, liver and bladder, bottom: coronal slices showing vena cava, aorta, iliac artery and right kidney.

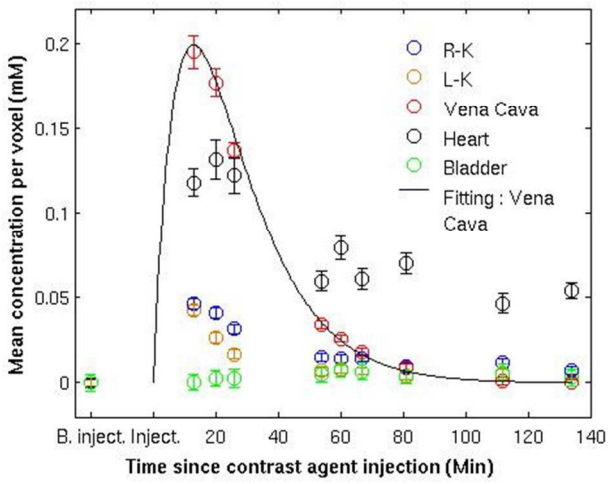

Figure 3. Time dependence of the $Gd^{3+}/[Fe(CN)_6]^{3-}$@D-mannitol concentration per voxel as a function of time per organ of interest (heart, bladder, kidney, vena cava). Solid line gives the fitting of the time-dependent evolution of Gd^{3+} concentration in blood in vena cava by using the bi-compartmental model.

To investigate the safety aspects related to the use of these nanoparticles for MRI, mice were injected intravenously with a NaCl aqueous solution containing the $Gd^{3+}/[Fe(CN)_6]^{3-}$@D-mannitol nanoparticles as a single dose four times greater than that used for MRI (*i.e.* 0.012 mmoles of Gd^{3+} per Kg). Sixteen days after injection, histological analysis revealed no apparent abnormalities or lesions on the heart, liver, spleen or kidneys (Fig. 4a). This result was confirmed by a stable concentration of conventional biomarkers that are representative of the functionality of the tissues and/or systemic inflammation such as ALT (liver function), creatinine (renal function), TNF-α and IL-6 (systemic toxicity) (Fig. 4b-e).[18] Then, routes of elimination and organ retention of the nanoparticles were measured by inductively coupled plasma mass spectrometry (ICP-MS). These analyses show that 0.3% of Gd^{3+} is excreted by urines in the first few

hours (not shown) and 19.5% in the faeces during the following days (Fig. 4f) whereas 20.7% is retained in the liver (Fig. 4g). This may be due to the involvement of blood and urinary pathways at the beginning of treatment and then to the relay of the metabolic pathway responsible for the retention of gadolinium in the liver and its continuous excretion in the faeces as was previously suggested by MRI monitoring. Note that after 16 days, we recovered nearly half of Gd^{3+} injected suggesting that it has still retained in other organs.

In conclusion, the use of $Gd^{3+}/[Fe(CN)_6]^{3-}$ nanoparticles stabilized by a biocompatible and soluble in water at physiological pH stabilizing agent seems to be a promising approach for the design intravascular nanoprobes for MRI. The paramagnetic $Gd^{3+}/[Fe(CN)_6]^{3-}$@D-mannitol nanoparticles of 3.41 nm exhibit high relaxivity with a r_1 value of 11.4 $mM^{-1}s^{-1}$ and a r_2/r_1 ratio close to 1 and thus can function as an efficient positive CA. The *in-vivo* MRI measurements demonstrate that these nanoparticles not only significantly enhance the MRI signal with a considerably lower dose in comparison with commercial Gd^{3+} chelates, but also have a prolonged intravascular circulation and may be considered as a rare example of CA based on nanoscale Prussian blue type coordination polymer network. Preliminary studies of nanoparticles clearance and toxicity performed in mice indicate that there are no systemic and organ toxicity associated with these nanoparticles 16 days post-injection with both, the glomerular and the blood pathway excretion at the beginning of the process. However a longer investigation must be conducted to determine the time required for the total elimination of nanoparticles. Thus, this study demonstrates that these nanoparticles are more efficient than commercial gadolinium-containing CAs such as Gd-DTPA not only because they exhibit a higher relaxivity but also because of their longer blood-circulation lifetime. It also provides an additional lane to the reflections conducted for the development of novel CAs at the nanoscale for MRI.

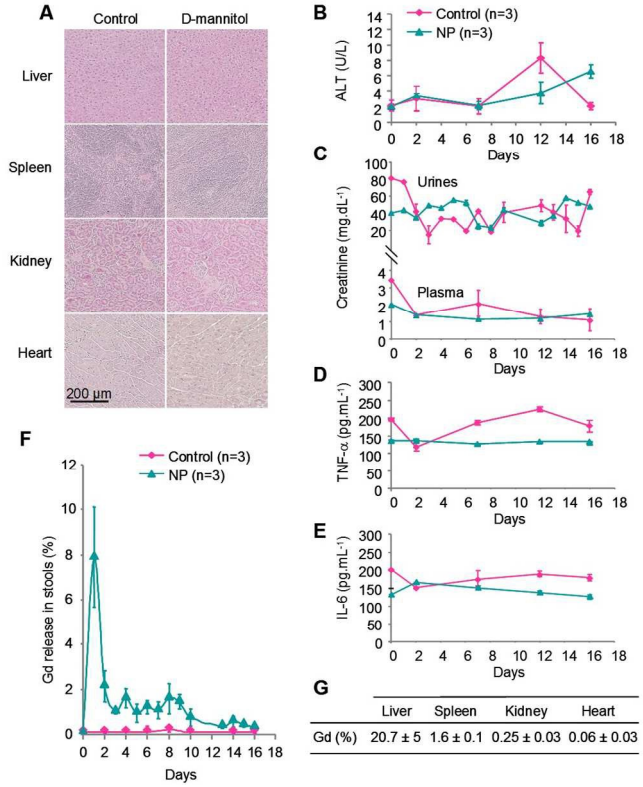

Figure 4. Biocompatibility and elimination of $Gd^{3+}/[Fe(CN)_6]^{3-}$@D-mannitol nanoparticles (NP). (A) Hematoxylin- and eosin-stained sections from paraffin-embedded tissues of control and treated mice. (B-E) Plasma or urine levels of biomarkers of liver (ALT), renal (creatinine) or systemic inflammation (TNFα, IL-6). (F) Elimination by stools of Gd^{3+} up to 16 days. (G) Gd^{3+} retention in liver, heart, kydney and spleen up to 16 days. Values are means ± standard deviation.

Acknowledgements

The authors are grateful to the ERA.NET-RUS project ST085 COPONAMRI, University of Montpellier and CNRS for financial support. We also thank PAC Chimie Balard and BionanoMRI platforms and R. Freydier and J. L. Seidel for ICP-MS analyses ("AETE" Analytical Regional Platform Facilities, OREME observatory of Montpellier).

Notes and references

[a]Institut Charles Gerhardt Montpellier (ICGM), UMR 5253, Ingénierie Moléculaire et Nano-Objets, Université de Montpellier, place Eugène Bataillon, Montpellier, France. E-mail: joulia.larionova@um2.fr.

[b]Institut des Biomolécules Max Mousseron, UMR5247, CNRS-UM1-UM2, Université de Montpellier, Faculté de Pharmacie, Avenue Charles Flahault, 34093 Montpellier Cedex 05, France. E-mail: magali.gary-bobo@inserm.fr.

[c]L2C, UMR 5221 CNRS-UM2, Equipe BioNanoNMRI, Université de Montpellier, Place Eugène Bataillon, 34095 Montpellier Cedex 5, France.

[d]PCB_Unit of Experimental Toxicology and Ecotoxicology (UTOX-PCB), Scientific Park of Barcelona 08028, Spain.

[e]Nuclear Medicine Department, Montpellier University Hospital, 80 avenue Augustin Fliche, 34080 MONTPELLIER Cedex 5, France.

Electronic Supplementary Information (ESI) available: experimental details and procedures, toxicological data, physical characterizations.

[f]NanoMedSyn, avenue Charles Flahault, 34093 Montpellier Cedex 05, France.

†These two authors contribute equally to this work.

1 a) M. Oh, C. A. Mirkin, *Nature* 2005, **438**, 651; b) S. Vaucher, M. Li, S. Mann, *Angew. Chem., Int. Ed.* 2000, **39**, 1793; c) L. Catala, F. Volatron, D. Brinzei, T. Mallah, *Inorg. Chem*. 2009, **48**, 3360; d) J. Larionova, Y. Guari, C. Sangregorio, Ch. Guérin, *New J. Chem*. 2009, **33**, 1177.

2 a) P. Horcajada, R. Gref, T. Baati, P. K. Allan, G. Maurin, P. Couvreur, G. Férey, R. E. Morris, Ch. Serre, *Chem. Rev*., 2012, **112**, 1232; b) K. M. L. Taylor, A. Jin, W. Lin, *Angew. Chem. Int. Ed*. 2008, **47**, 7722.

3 a) G. Férey, C. Mellot-Draznieks, C. Serre, F. Millange, J. Dutour,S. M. Surblé, I. Margiolaki, *Science*, 2005, **309**, 2040 ; b) G. Férey, C. Serre, C. Mellot-Draznieks, F. Millange, S. Surblé, *Angew. Chem., Int. Ed*., 2004, **116**, 6456; c) B. B. Yang, R. B. Abel, A. C. G. Upruchard, J. A. Smithers, S. T. Forgue, *J. Clin. Pharmacol*., 1996, **36**, 623; d) K. M. L. Taylor-Pashow, J. Della Rocca, Z. Xie, S. Tran, W. Lin, *J. Am. Chem. Soc*. 2009, **131**, 14261 ; e) S. R. Miller, D. Heurtaux, T. Baati, P. Horcajada, J.-M. Grenèche, C. Serre, *Chem. Commun*. 2010, **46**, 4525; f) G. Férey, C. Mellot-Draznieks, C. Serre, F. Millange, J. Dutour, S. M. Surblé, I. Margiolaki, *Science* 2005, **309**, 2040 ; g) G. Férey, C. Serre, C. Mellot-Draznieks, F. Millange, S. Surblé, *Angew. Chem., Int. Ed.* 2004, **116**, 6456; g) F Ke, Y.-P. Yuan, L.-G. Qiu, Y.-H. She, A.-J. Xie, J.-F Zhu, X.-Y. Tian, L.-D. Zhang, *J. Mater. Chem*. 2011, **21**, 3843; h) S. R. Miller, D. Heurtaux, T. Baati, P. Horcajada,

J.-M. Grenèche, C. Serre, *Chem. Commun*. 2010, **46**, 4525 ; l) H.-Y. Lian, M. Hu, Ch-H. Liu, Y. Yamauchi, C.-W. Wu *Chem. Commun*. 2012, **48**, 5151.

4 (a) G. Fu, W. Liu, S. Feng, X. Yue, *Chem. Commun*., 2012, **48**, 11567; (b) M. S. Kandanapitiye, F. J. Wang, B. Valley, C. Gunathilake, M. Jaroniec, S. D. Huang, *Inorg. Chem*. 2014, **54**, 1212; (c) H. A. Hoffman, L. Chakrabarti, M. F. Dumont, A. D. Sandler, R. Fernandes *RSC Adv*. 2014, **4**, 29729; (d) G. Fu, W. Liu, Y. Li, L. Jiang, X. Liang, Sh. Feng, Z. Dai, *Bioconjugate Chem.* 2014, **25**, 1655.

5 a) M. Perrier, M. Busson, G. Massasso, J. Long, V. Boudousq, J.-P. Pouget, S. Peyrottes, Ch. Perigaud, C. Porredon-Guarch, J. de Lapuente, M. Borras, J. Larionova, Y. Guari, *Nanoscale*, 2014, **6**, 13425; b) V. S. Perera, J. Hao, M. Gao, M. Gough, P. Y. Zavalij, C. Flask, J. P. Basilion, S. D. Huang, *Inorg. Chem*., 2011, **50**, 7910; c) K. E. deKrafft, Z. Xie, G. Gao, S. Tran, L. Ma, O. Z. Zhou, W. Lin, *Angew. Chem. Int. Ed*., 2009, **48**, 9901; d) X. Liang, Z. Deng, L. Jing, X. Li, Z. Dai, C. Li, M. Huang, *Chem. Commun*. 2013, **49**, 11029; e) L. Jing, X. Liang, Z. Deng, S. Feng, X. Li, M. Huang, C. Li, Z. Sai, *Biomaterials*, 2014, **35**, 5814.

6 a) K. M. L. Taylor, W. J. Rieter, W. Lin, *J. Am. Chem. Soc*., 2008, **130**, 14358; b) G. A. Pereira, J. A. Peters, F. A. Almeide Paz, J. Rocha, C. F. G. Geraldes, *Inorg. Chem*., 2010, **49**, 2969; b) K. M. L. Taylor, A. Jin, W. Lin, *Angew. Chem., Int. Ed*., 2008, **47**, 7722; c) W. J. Rieter, K. M. Pott, K. M. L. Taylor, W. Lin, *J. Am. Chem. Soc*., 2008**, 130**, 11854; d) P. Horcajada, T. Chalati, Ch. Serre, B. Gillet, C. Sebrie, T. Baati, J. F. Eubank, D. Heurtaux, P. Clayette, Ch. Kreuz, J.-S. Chang, Y. K. Hwang, V. Marsaud, Ph.-N. Bories, L. Cynober, S. Gil, G. Férey, P. Couvreur, R. Gref, *Nature Materials*, 2010, **9**, 172; e) P. Horcajada, Ch. Serre, G. Maurin, N. A. Ramsahye, F. Balas, M. Vallet-Regí, M.Sebban, F. Taulelle, G. Férey, *J. Am. Chem. Soc*., 2008, **130**, 6774; f) A. C. McKinlay, R. E. Morris, P. Horcajada, G. Ferey, R. Gref, P. Couvreur, Ch. Serre, *Angew. Chem. Int. Ed*., 2010, **49**, 6260; g) K. M. L. Taylor, W. J. Rieter, W. Lin, *J. Am. Chem. Soc*., 2008, **130**, 14358; h) G. Paul, Y. Prado, N. Dia, E. Rivière, S. Laurent, M. L. Vander Elst, R. N. Muller, L. Sancey, P. Perriat, O. Tillement, T. Mallah and L. Catala, *Chem. Commun*., 2014, **50**, 6740; i) M. F. Dumont, H. A. Hoffman, P. R. S. Yoon, L. S. Conklin, S. R. Saha, J. P. Paglione, R. W. Sze, R. Fernandes, *Bioconjugate Chem.* 2014, **25**, 129.

7 J. L. Bridot, A. C. Faure, S. Laurent, C. Riviere, C. Billotey, B. Hiba, M. Janier, V. Josserand, J. L. Coll, L. Vander Elst, R. Muller, S. Roux, P. Perriat, O. Tillement, *J. Am. Chem. Soc*., 2007, **129**, 5076.

8 a) J. Y. Park, M. J. Baek, E. S. Choi, S. Woo, J. H. Kim, T. J. Kim, J. C. Jung, K. S. Chae, Y. Chang, G. H. Lee, *ACS Nano*, 2009, **3**, 3663; b) M. Ahren, L. Selegard, A. Klasson, F. Soderlind, N. Abrikossova, C. Skoglund, T. Bengtsson, M. Engstrom, P. O. Kall, K. Uvdal, *Langmuir*, 2010, **26**, 5753.

9 H. Hifumi, S. Yamaoka, A. Tanimoto, T. Akatsu, Y. Shindo, A. Honda, D. Citterio, K. Oka, S. Kuribayashi, K. Suzuki, *J. Mater. Chem*., 2009, **19**, 6393.

10 E. J. Lee, W. C. Heo, J. W. Park, Y. Chang, J.-E. Bae, K. S. Chae, T. J. Kim, J. A. Park, G. H. Lee, *Eur. J. Inorg. Chem*., 2011, **16**, 2858.

11 a) S. D. Huang, Y. Li, M. Shokouhimehr, US Patent US20090384391 20090403, 2010; b) Y. LI, C. Li and D.R. Talham*, Nanoscale*, 2015, DOI: 10.1039/C4NR06481J.

12 V. S. Perera, L. D. Yang, J. Hao, G. Chen, B. O. Erokwu, C. A. Flask, P. Y. Zavalij, J. P. Basilion, S. D. Huang, *Langmuir* 2014, **30**, 12018.

13 Y. Guari, J. Larionova, M. Corti, A. Lascialfari, M. Marinone, G. Poletti, K. Molvinger, Ch. Guérin, *Dalton Trans*., 2008, 3658.

14 E. Chelebaeva, J. Larionova, Y. Guari, R. A. S. Ferreira, L. D. Carlos, A. A. Trifonov, T. Kalaivani, A. Lascialfari, Ch. Guérin, K. Molvinger, L. Datas, M. Maynadier, M. Gary-Bobo, M. Garcia, *Nanoscale*, 2011, **3**, 1200.

15 M. Perrier, S. Kenouch, J. Long, K. Thangavel, J. Larionova, Ch. Goze-Bac, A. Lascialfari, M. Mariani, N. Baril, Ch. Guérin, B. Donnadieu, A. Trifonov, Y. Guari, *Inorg. Chem*., 2013, **52**, 13402.

16 X. Zhou, W.-T. Wong, M. D. Faucher, P. A. Tanner *J. Solid State Chem*., 2008, **181**, 3057.

17 G. Liang, D. Ye, X. Zhang, F. Dong, H. Chen, S. Zhang, J. Li, X. Shen, J. Kong, *J. Mater. Chem. B* 2013, **1**, 3545.

18 M. Gary-Bobo, Y. Mir, C. Rouxel, D. Brevet, I. Basile, M. Maynadier, O. Vaillant, O. Mongin, M. Blanchard-Desce, A. Morère, M. Garcia, J. O. Durand, L. Raehm, *Ange. Chem. Int. Ed. Engl.,* 2011, **50**, 11425.